International Journal of Solids and Structures xxx (xxxx) xxx

Contents lists available at ScienceDirect

International Journal of Solids and Structures

journal homepage: www.elsevier.com/locate/ijsolstr

An assessment of discrete element approaches to infer intergranular forces from experiments on 2D granular media

M. Tolomeo[a,*], V. Richefeu[a], G. Combe[a], J.N. Roux[b], G. Viggiani[a]

[a] Univ. Grenoble Alpes, CNRS, Grenoble INP, 3SR, F-38000, Grenoble, France
[b] Université Paris-Est, Laboratoire Navier, 2 Allée Kepler, Cité Descartes, Champs-sur-Marne 77420, France

ARTICLE INFO

Article history:
Revised 7 November 2018
Available online xxx

Keywords:
Granular media
Contact forces
Discrete element method
Non-smooth contact dynamics
Image analysis

ABSTRACT

We propose a new way to estimating interparticle contact forces in granular materials, based on the combination of experimental measurements and numerical techniques that take the contact laws respectively from Molecular Dynamics and Non-Smooth Contact Dynamics discrete element methods. Tests are performed in quasi-static conditions on a two-dimensional granular assembly; 80 MPixel pictures of the assembly are shot throughout each test. Image processing and Digital Image Correlation are used in order to get information on the geometry of the assembly (particles and contact points position) and the rigid-body motion of particles (displacements and rotation); based on this information, numerical methods can be applied to assess contact forces. 2D DEM simulations are also performed and the same information is extracted and used for contact force estimation, so that the numerical methods can be validated. The reproducibility of the original set of contact forces is shown to be dependent on the displacement history for the first method, based on contact elasticity, and on the degree of force indeterminacy for the Contact Dynamics-based one. The validation phase also includes a perturbation analysis to predict the influence of measurement error (bad contact detection) when applying the Contact Dynamics-based method, which shows the robustness of this method. After this validation phase, the methods are applied to experimental data. Measurement error on kinematic measurements turns out to be quite significant for the first approach, while it does not affect the second, for which the accuracy of the force estimation can be assumed to be mainly dependent on the degree of force indeterminacy of the system.

1. Introduction

Granular matter constitutes a very broad category of materials, that can be found in nature as well as in several industrial applications (*e.g.*, pharmaceutical). The great research interest in their behaviour is also due to their discrete nature, that makes the typical continuum mechanics unable to describe some aspects of their behaviour. One of these aspects is the way contact forces are transmitted in a granular assembly. Understanding the mechanisms of force transmission between grains is not only important for the sake of building physically-based constitutive models; it is also fundamental to study phenomena such as grain crushing (Doreau-Malioche et al., 2018; Karatza et al., 2017). Dantu (1957) first highlighted the strong heterogeneity and anisotropy in contact forces distribution through photoelastic experiments. Discrete Element Methods (Cundall and Strack, 1979) allowed modelling an assembly of grains as a system of individual bodies governed by the equations of dynamics; this made it possible to access the extremely rich information at the microscale of granular assemblies, study the force heterogeneity in depth and link it with the macroscopic behaviour (Radjai et al., 1996, 1998).

While numerical simulations give access to both particle displacements and interparticle contact forces, the determination of the latter from experiments still remains a challenge. To this purpose, some techniques have already been proposed, though limited by some constraints: among them, a fully experimental one uses carbon paper to show the print of normal forces at the boundaries of a bead packing (Mueth et al., 1998). Other methods combine experimental measurements with numerical approaches. Among these, through photoelasticity (Dantu, 1957; Majmudar and Behringer, 2005) it is possible to highlight stress patterns in an assembly of birefringent grains, and consequently infer contact forces based on assumptions on the constitutive behaviour of the material. The Granular Element Method (Andrade and Avila, 2012; Hurley et al., 2014; Marteau and Andrade, 2017) combines average grain strain measurements with basic Newtonian mechanics and an optimisation problem to infer forces. A similar approach was

* Corresponding author.
E-mail address: mathias.tolomeo@3sr-grenoble.fr (M. Tolomeo).

https://doi.org/10.1016/j.ijsolstr.2019.01.010
0020-7683/

also developed on the basis of 3D X-ray diffraction and X-ray computed tomography measurements (Hurley et al., 2016).

In the same philosophy of these methods, we propose an approach that indirectly estimates forces based on experimental measurements. In particular, we aim for a simple method, based on few input data, and independent of the used material. To this purpose, we focus on the rigid body motion (displacements, rotation) of particles in a two-dimensional assembly. From the knowledge of the external loading and particle positions during time we apply two different numerical approaches to infer contact forces. We show that both methods, despite some limitations that are observed, might represent promising tools for a realistic assessment of contact forces.

The paper is structured in the following way: in Section 2 we present the two numerical approaches, whose validation on an ideal experiment (MD simulation) is in Section 3; in Section 4 we show results from applications to real experimental data; finally, Section 5 is dedicated to some concluding remarks.

2. Methodology

The idea of using experimental measurements and applying the DEM framework to estimate contact forces is common to the two proposed methods. However, the methods are quite different from each other. The first one is based on Molecular Dynamics force laws; it makes a direct estimation of forces based only on the measured kinematics, by exploiting the local elasticity at the contact scale. Hence, it is referred to as contact elasticity method (CEM). The second one, referred to as Contact Dynamics-based method (CDM), is based on Non-Smooth Contact Dynamics that neglects such length scale, assuming perfectly rigid bodies and imposing that no particle interpenetration occurs. This results in a non-uniqueness of CDM's solution, that is related to the degree of force indeterminacy of the system; such a solution has to be obtained through a numerical resolution. On the other hand, the solution in terms of forces estimated through the CEM is unique. A possible application is to combine the two methods by injecting part of the CEM solution (*e.g.*, normal forces) in the numerical resolution of the CDM to find the remaining part; this way, by reducing the number of variables of the problem, we are basically re-introducing the initially neglected local elasticity in the CDM, hence eliminating the non-uniqueness of the solution.

The difference in the formulation of the two methods also entails a difference in the required information. In general, for both methods it is necessary to define the contact network (contact point locations and branch vector orientations) and the boundary conditions (external loading); in addition, the CEM requires the definition of contact kinematics – typically inferred from particle kinematics – as it deals with evolutions between two granular states. The CDM, on the contrary, can provide an estimation of forces for a single state for which only the contact network and boundary conditions are known.

2.1. Contact elasticity method (CEM)

The first proposed method, referred to as contact elasticity method (CEM), aims to directly infer forces from the kinematic measurements, in particular from contact relative displacements. To this end, some appropriate force laws have to be introduced, together with the parameters that appear in them. Based on the common Molecular Dynamics (MD) force laws (Cundall and Strack, 1979), normal forces are assumed to be only repulsive, and linear with the overlap δn through the contact normal stiffness k_n; as for tangential forces, they are incrementally linear with the tangential relative displacement $v_t\,\delta t$ through the contact tangential stiffness k_t, with the constraint given by Coulomb friction, that requires them to fall within the range $[-\mu f_n : \mu f_n]$. Therefore, tangential forces are determined as a sum of force increments; this introduces a dependency on the displacement history, and so on the time resolution of the data acquisition.

$$\begin{cases} f_n = k_n\ \delta n \\ \delta f_t = k_t\ v_t\ \delta t \end{cases} \tag{1}$$

2.2. Contact dynamics-based method (CDM)

In Non-Smooth Contact Dynamics (NSCD), contact laws are expressed as complementarity relations, that respectively require forces to prevent particle interpenetration (Signorini condition) and implement Coulomb friction (Radjai and Richefeu, 2009; Moreau, 2004). In this method, the elastic length scale – associated with contact deflection – is neglected, as particles are assumed to be rigid, so that forces do not have to be resolved during a collision: one simply calculates post-collisional velocities as a function of pre-collisional ones (McNamara and Herrmann, 2004).

Our application of the NSCD framework to experimental data aims to solve the Gauss-Seidel iterator that typically starts from a set of zero-forces, although initialising it with a guess solution closer to the expected one may facilitate the convergence to a solution. As a result of the Gauss-Seidel iterator, a set of contact forces is obtained for a given configuration of the system (*i.e.*, for a given external loading and geometrical arrangement, extracted from one of the pictures taken during the tests).

While the CEM simply estimates forces from displacements, with no limitation (except for cutting tangential forces if they violate the Coulomb condition), with the CDM we inject the equations of motion, and so the mechanics of the system; we therefore obtain a *mechanically admissible* solution. If we approach quasi-static loading conditions, in principle (assuming the contact network is correctly defined) the CDM will find a set of contact forces close to static equilibrium.

As previously mentioned, a possible application of these methods is a combination of the two of them: the CDM can benefit from starting the Gauss-Seidel iterator with an initial guess solution more or less realistic: to this end, the output of the CEM (or part of it) can be used. Typically, one could think of using normal forces, in order to exploit the local elasticity (that the CDM neglects); however, also tangential forces could be used, if their estimation is reputed to be more reliable than that of normal forces.

3. Validation

Before applying the two numerical approaches to an experimental case, a validation phase is carried out by working on three MD simulations. In order to reproduce the experimental conditions as in Section 4, we try to reconstruct the force network in the simulations by using the same information as what we would get from the experiments, *i.e.*, boundary conditions, geometry of the packing (contact network) and, for the CEM, particle motion. Similarly to the experimental application, in which measurements are discrete-in-time as they come from pictures of the assembly that are generally shot every 5 s, we take this input data from snapshots of the assembly during the simulations, with a constant vertical strain $\Delta\varepsilon_{yy} = 2 \times 10^{-5}$ between two consecutive snapshots.

We refer to these simulations as "ideal" experiments, since we benefit from the fact of having no measurement error, differently from the real experimental case; at the same time, since the contact forces at any stage of the simulations are known, we can test the success of the numerical methods of force inference by comparing the estimated set of forces with the actual one, taken as "ground truth". A possible way of carrying out this comparison is

Please cite this article as: M. Tolomeo, V. Richefeu and G. Combe et al., An assessment of discrete element approaches to infer intergranular forces from experiments on 2D granular media, International Journal of Solids and Structures, https://doi.org/10.1016/j.ijsolstr.2019.01.010

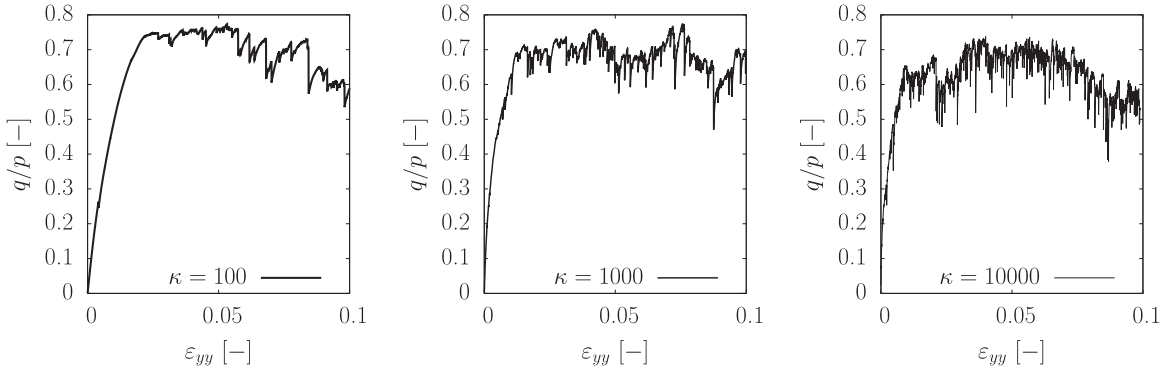

Fig. 1. Stress-strain curves for the three biaxial vertical MD simulations, for $\kappa = 100,\ 1000,\ 10000$ respectively, with the ratio between the deviatoric invariant q and pressure p on the y-axis.

the computation of Pearson's correlation coefficient r between the two sets of forces (generally separating normal forces from tangential forces). Given two datasets $\{x_1, \ldots, x_n\}$ and $\{y_1, \ldots, y_n\}$ – the two sets of forces –, r lies in the range $[-1 : 1]$, where 1 is total positive linear correlation, 0 is no linear correlation, and -1 is total negative linear correlation; it takes the following expression:

$$r = \frac{\sum_{i=1}^{n}(x_i - \bar{x})(y_i - \bar{y})}{\sqrt{\sum_{i=1}^{n}(x_i - \bar{x})^2}\sqrt{\sum_{i=1}^{n}(y_i - \bar{y})^2}} \tag{2}$$

where n is the sample size (number of contacts), x_i and y_i are individual members of each sample (*i.e.*, values of single contact force components) and $\bar{x}$, $\bar{y}$ are their respective mean values.

The three biaxial vertical compression MD simulations were carried out by applying a constant deformation rate $\dot{\varepsilon}_{yy}$ on an assembly of 1852 frictional disks with four different diameters. The number of constituents and size for each class resemble those in the experiments on wooden cylinders in Section 4. The four diameters have a ratio with the largest one of 0.4, 0.6, 0.7 and 1.0, and the number of disks per class is 797, 425, 406 and 224, respectively. The stress-strain response is shown in Fig. 1, in terms of the ratio between the stress deviator $q = (\sigma_1 - \sigma_2)$ and mean normal stress $p = .5\ (\sigma_1 + \sigma_2)$. Particle-particle and particle-wall friction coefficients were respectively set to 0.5 and 0; no gravity was acting on the particles. Before performing biaxial compression, in the three simulations the assembly was isotropically compressed up to different values of pressure ($p = 5,\ 50,\ 500$ kPa, respectively), so that the initial stiffness level, with a constant contact normal stiffness $k_n = 5 \times 10^7$ N/m, was $\kappa = k_n/p = 100,\ 1000,\ 10000$, respectively.

3.1. Contact elasticity method (CEM)

We apply the CEM by measuring contact relative displacements between geometrical configurations taken as distinct snapshots of the three MD biaxial vertical compression simulations, and inferring contact forces through the application of the contact laws in Eq. 1.

With respect to the computation of normal forces, contact elasticity can be easily exploited by measuring particle interpenetration, so that the real forces are perfectly retrieved; in contrast, the estimation of tangential forces is affected by the influence of displacement history, since we assume an incremental contact law. The effect of this can be assessed by changing the time resolution – or, equivalently, the width of the corresponding strain window, since a constant strain rate is imposed – and looking at how the accuracy of the tangential forces estimation changes. In Fig. 2a, Pearson's r between estimated and reference normal forces is plotted for all states in the simulation with intermediate κ. Each curve corresponds to an application of the CEM with a different size of the strain window between two consecutive states. A clear decrease in the correlation between the estimated tangential forces and the reference ones is observed as the strain window is enlarged. The drops observed in most of the curves are caused by large grain rearrangements and restructuring of the contact network occurring in the reference simulation, typically corresponding to the stress relaxations observed in Fig. 1.

Another typical feature when dealing with frictional packings is the memory of previously accumulated tangential forces: in a real case, one might assume that some friction at the contact level already developed before the measurements start; in order to assess the effect of this, we compared the estimation of tangential forces, for the same strain window (*i.e.*, the smallest possible one), when taking into account previously accumulated forces (here, forces that developed during a previous phase of isotropic compression up to the desired confining stress) and when neglecting them. It is shown (Fig. 2b) that this difference decays quite fast, as the two curves get closer to each other; however, it takes a significant deformation ($\varepsilon_{yy} \approx 10\%$) until the effect of memory is completely lost and the two curves overlap.

Fig. 3 shows the influence of the stiffness level κ on the accuracy of tangential force estimation. In order to separate its influence from the effect of the strain window, the same strain window $\Delta\varepsilon_{yy} = 2 \times 10^{-5}$ is adopted for all simulations corresponding to different κ. It is observed that, in the first phase – in which little or no granular rearrangement occurs – the estimation is more accurate for higher κ. In a second phase, rearrangement occurs and becomes more intense as κ grows; due to this, larger drops in the evolution of r are observed for higher κ. Despite these differences, on average all three curves seem to stabilise around a value of $r \approx 0.9$ towards the end of the simulation.

3.2. Contact dynamics-based method (CDM)

Similarly to the first method, the CDM was applied by running the Gauss-Seidel iterator on the same geometrical configurations extracted from the above-mentioned MD simulations.

By assuming grains to be rigid, the elastic length scale associated with contact deformation is neglected; this results in the loss of uniqueness of the solution: the set of contact forces obtained through the CDM is only one of the possible contact states. This force ensemble can be easily explored for a small system in order to estimate its amplitude (McNamara and Herrmann, 2004; Unger and Kertèsz, 2003); it can be shown that the variability of contact forces between all possible solutions is somehow limited.

The amplitude of the force ensemble is directly linked to other parameters typically used to describe properties of the geometrical arrangement, such as the coordination number and the degree of

Please cite this article as: M. Tolomeo, V. Richefeu and G. Combe et al., An assessment of discrete element approaches to infer intergranular forces from experiments on 2D granular media, International Journal of Solids and Structures, https://doi.org/10.1016/j.ijsolstr.2019.01.010

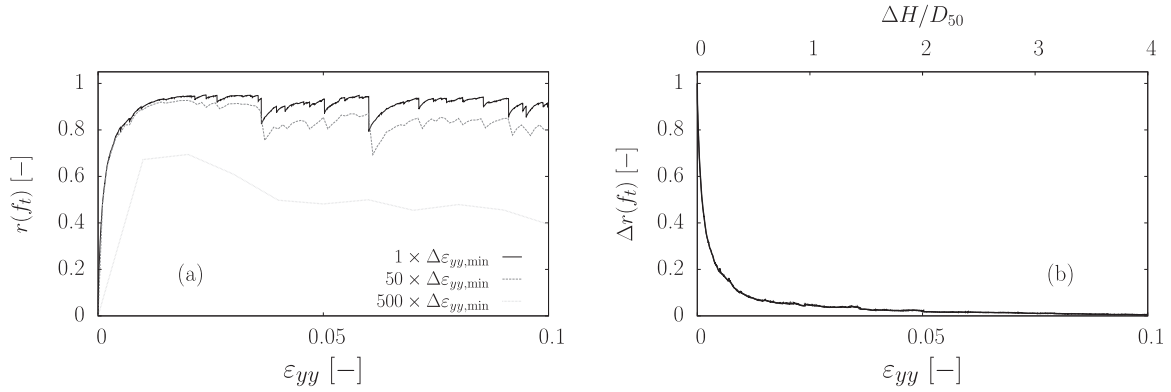

Fig. 2. (Left) Evolution of Pearson's r for tangential forces, between the CEM solution and the original set of forces, for different widths of the strain window (here expressed in terms of the smallest one, corresponding to a strain increment $\Delta\varepsilon_{yy} = 2 \times 10^{-5}$). The stiffness level κ is 1000. Tangential forces accumulated in the previous isotropic compression phase are neglected. The accuracy of tangential forces estimation is shown to be decreasing as the size of the strain window increases. (Right) Evolution of the difference between two curves corresponding to a strain window of $1 \times \Delta\varepsilon_{yy,\,\min}$, respectively obtained by neglecting previously accumulated tangential forces (darker curve on the left) and by taking them into account. The evolution is also expressed in terms of the displacement applied to the wall, normalised by the D_{50} of the assembly, showing that, despite the fast decay of the difference, the effect of memory is still not completely lost up to a displacement of 4 times the D_{50}.

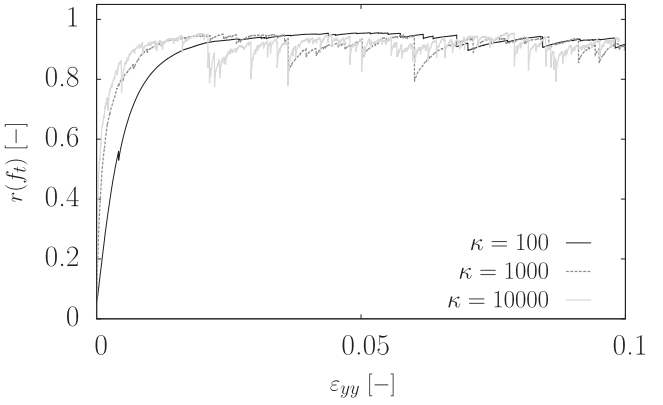

Fig. 3. Evolution of Pearson's r for tangential forces, between the CEM solution and the original set of forces, for initial stiffness levels $\kappa = 100$, 1000 and 10000. All curves are obtained with the same strain window $\Delta\varepsilon_{yy} = 2 \times 10^{-5}$. Tangential forces accumulated in the previous isotropic compression phase are neglected.

Table 1
Main characteristics of the initial states of MD simulations prepared with different stiffness level κ: packing fraction ϕ, coordination number z (*i.e.*, number of contacts per particle), degree of hyperstaticity h (as defined by Eq. 3) and the ratio of *rattlers* (*i.e.*, "floating" grains not involved in any contact) to the total number of grains. There is a clear increase of the degree of hyperstaticity h as the stiffness level κ decreases.

κ	ϕ	z	h	Rattlers [%]
100	0.848	3.78	1601	4.2
1000	0.828	2.81	409	15.5
10000	0.825	2.56	196	19.7

hyperstaticity (force indeterminacy) h, that can be derived from the following relation (Roux and Combe, 2011):

$$N_l + h = D\ N_c + k \tag{3}$$

being N_l the number of degrees of freedom of the system (3 for each particle in 2D), D the dimension of the system, N_c the number of contacts and k the degree of hypostaticity (velocity indeterminacy). The degree of hypostaticity k is the dimension of the set of particle displacements and rotations that do not induce any contact relative displacement (also referred to as *mechanisms*); in the absence of gravity, such displacements correspond to the degrees of freedom associated with "floating" grains that are not in contact with any other grain (*rattlers*).

These quantities are summarised in Table 1 for the three simulations. It is clearly observed that force indeterminacy is higher for low values of the initial stiffness level. It is important to keep in mind that indeterminacy is also affected by interparticle friction, although its effect was not analysed here as μ was kept constant in these simulations: in particular, it was shown (Roux, 2000) that indeterminacy vanishes (*i.e.*, contact forces are uniquely determined) in frictionless granular assemblies, as the system becomes isostatic.

By applying the CDM to synthetic (MD) data, it is observed that the accuracy of the solution obtained, *i.e.*, the correspondence between the estimated set of forces and the original (MD) one, strongly depends on the degree of hyperstaticity of the system; in particular, a better correlation is systematically found for stiffer materials that, for the same loading conditions, exhibit a lower density, coordination number and degree of hyperstaticity (Fig. 4a), thus indicating that there might be a correlation between the degree of hyperstaticity and the variability of the solution in forces.

This result is confirmed by defining the error on normal force, for each contact, as the absolute difference between the estimated normal force and the real one, normalised by the average normal force; for a single contact state (close to isotropic compression, $\varepsilon_{yy} \approx 0$), the average value of the error is 0.427, 0.264, 0.211 and its variance equal to 0.364, 0.248, 0.208 for $\kappa = 100$, 1000 and 10000 respectively, while the complete distribution function is showed in Fig. 4b.

Since the non-uniqueness of the solution comes from an excess in the number of unknowns of the problem, with respect to the number of equations to solve it, a way of limiting its effect lies in the possibility of removing a certain number of variables. Being able to access the solution in forces of the DEM simulations, part of this solution can be used to assign constant values to the corresponding variables, so that only the remaining part has to be estimated: in particular, we can alternatively fix normal forces to prescribed values while estimating tangential ones, and opposite. The result of this operation is shown in Fig. 5. When all forces – normal and tangential – are estimated starting from an initial guess with only null forces (Fig. 5a), the correlation is around 0.9 for normal forces and 0.8 for tangential forces. Fig. 5b shows that imposing normal forces implies $r \approx 1$ for tangential forces, and vice-versa.

Before moving to the application to the experimental case, in which measurement error might have an important effect on the estimation of forces, a preliminary estimation of such effect was done by artificially perturbing the information extracted from the

Please cite this article as: M. Tolomeo, V. Richefeu and G. Combe et al., An assessment of discrete element approaches to infer intergranular forces from experiments on 2D granular media, International Journal of Solids and Structures, https://doi.org/10.1016/j.ijsolstr.2019.01.010

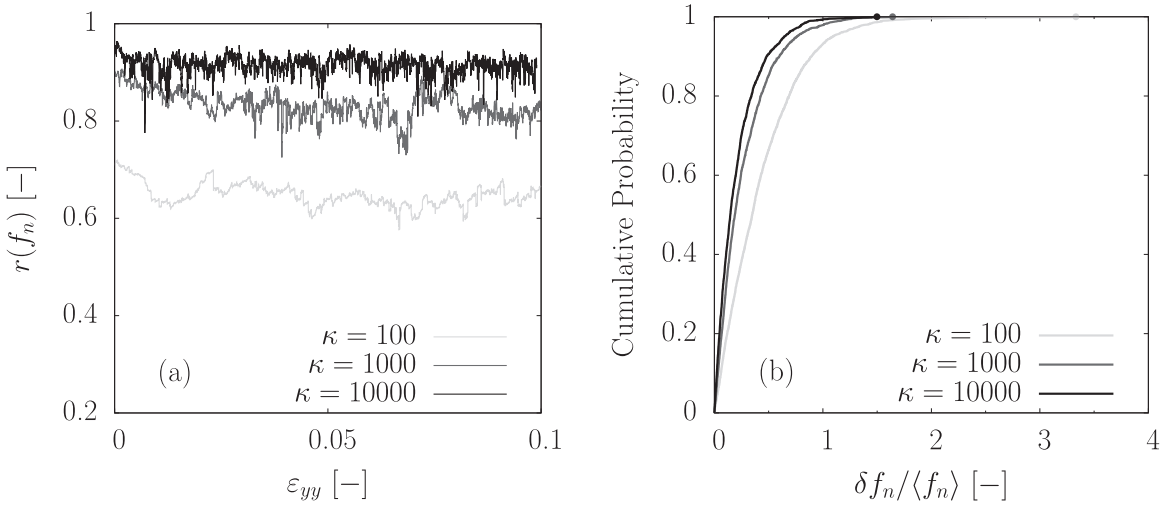

Fig. 4. (Left) Evolution of Pearson's r for normal forces in the three MD simulations (for $\kappa = 100, 1000, 10000$ respectively), between the solution estimated via the CDM and the real one. (Right) Cumulative Distribution Function of normal force error – defined as the absolute normal force difference normalised by the average normal force – for all contacts in a state at the early stage of the three MD simulations (close to isotropic compression conditions). It is shown here that the estimation of forces is more accurate as the stiffness of the material increases, as expected since stiffer materials typically show a lower degree of force indeterminacy.

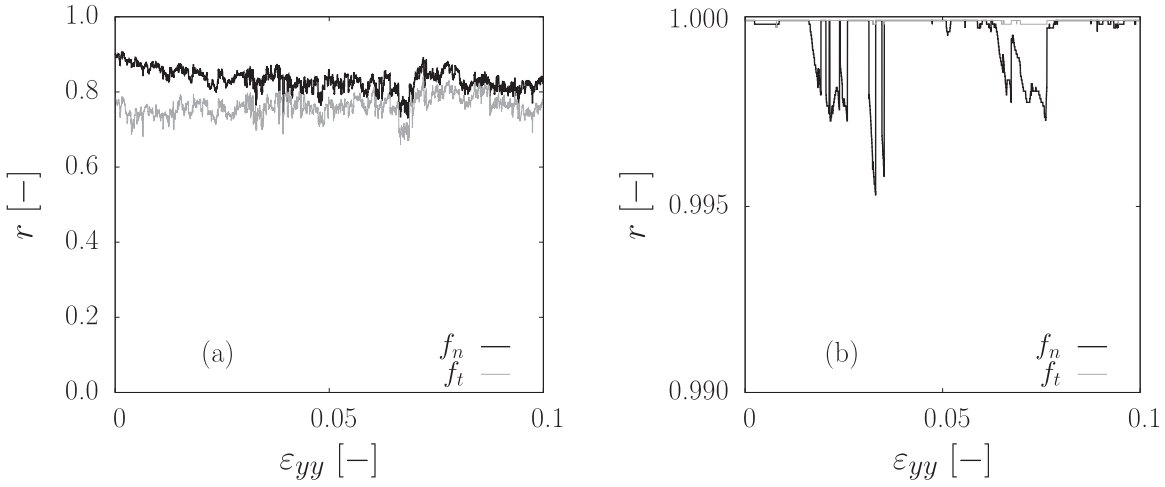

Fig. 5. (Left) Evolution of Pearson's r for normal and tangential forces, between the CDM solution and the original set of forces. The stiffness level κ is 1000. (Right) Evolution of Pearson's r, respectively for tangential forces f_t when imposing normal forces to be constant and equal to their original values, and for normal forces f_n when tangential ones are imposed, between the CDM solution and the original set of forces. The stiffness level κ is 1000. We show here that, when part of the unknowns of the system are eliminated by being assigned their original values, the correlation between the remaining part of forces and the original ones dramatically increases (Pearson's $r \approx 1$).

MD simulations, in order to see how the accuracy of the solution is affected by such error.

For the CDM case, since we only use boundary conditions and contact network as input information (no particle displacement or rotation), the main error could come from a possible bad detection of contacts. By tuning the threshold distance between two grains that defines whether they are in contact or not, it is possible to either increase or decrease the number of contacts; as the contact network changes, the effect is studied, for a single contact state, by comparing those contact forces that are common between the original contact network and the modified one (Fig. 6). It is observed that, for the three different κ, correlation of normal forces generally stays unchanged up to an error – in both directions – of about $4-5\%$ of the total number of contacts; the sudden drop is observed for an error larger than 10%, which is considerably higher than the error we assume we are making when detecting contacts from pictures of the assembly in real experiments. Focusing on single states, additional results can confirm this. The comparison of normal force maps shows that the main force chains are perfectly retrieved even with a bad contact detection, and it already gives a clue of how, for the case of an overestimated number of contacts, the added ones mainly carry below average (weak) normal forces (Fig. 7). This is finally proven by the statistics of such forces (Fig. 8), showing that, although this tendency is more evident for the lowest indeterminacy ($\kappa = 10000$), it is common to all simulations.

4. Application to experimental data

4.1. Experimental campaign

A number of tests were performed in the $1\gamma 2\varepsilon$ shear device (Calvetti et al., 1997; Joer et al., 1992). This machine can quasi-statically strain a two-dimensional model assembly of particles with independent control on the three components of the strain tensor $\varepsilon_{xx}, \varepsilon_{yy}$ and ε_{xy} (or γ); at the same time, it allows stress-controlled tests. The two-dimensional character of the problem is well attained especially in terms of stress, since no loading is applied on the two free surfaces of the specimen (the frontal and back surface referring to Fig. 9); out-of-plane deformations can

Please cite this article as: M. Tolomeo, V. Richefeu and G. Combe et al., An assessment of discrete element approaches to infer intergranular forces from experiments on 2D granular media, International Journal of Solids and Structures, https://doi.org/10.1016/j.ijsolstr.2019.01.010

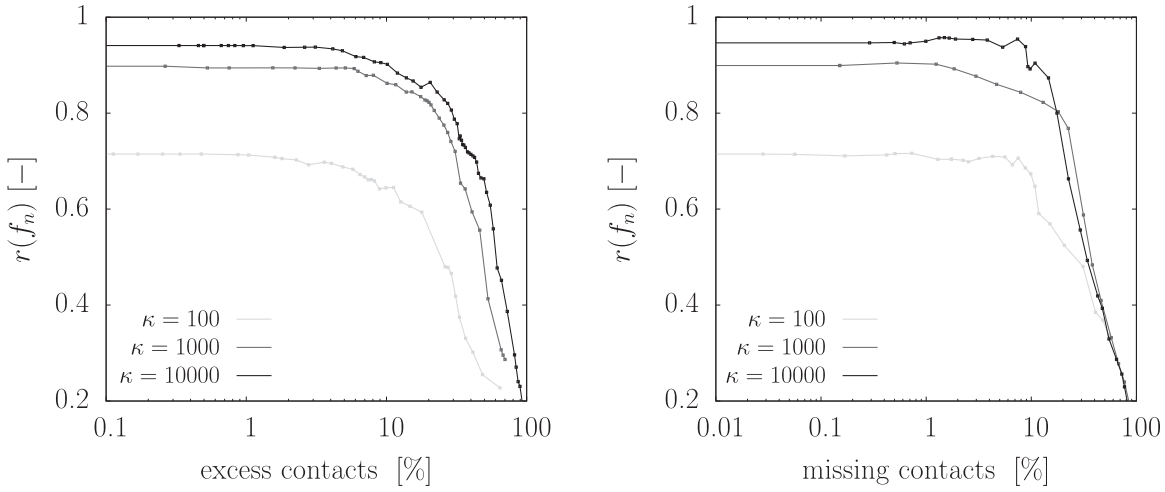

Fig. 6. Evolution of Pearson's r as the number of contacts is artificially increased (left) or decreased (right), for a state in the early stage of the simulations ($\varepsilon_{yy} \approx 0$, close to isotropic compression conditions), in the CDM solution. Excess (missing) contacts are expressed as the increase (decrease) in the total number of contacts normalized by the initial value. It is observed that the effect on the estimation of forces is negligible up to an error $\approx 5\%$ of the total number of contacts.

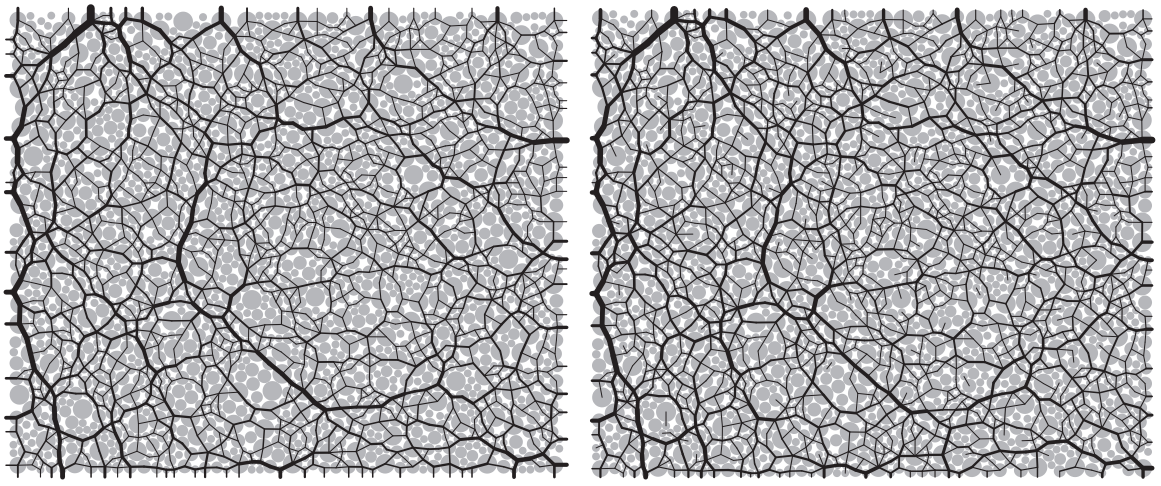

Fig. 7. (Left) Map of original (MD simulation) normal forces from an early state ($\varepsilon_{yy} \approx 0$) of a biaxial vertical compression with $\kappa = 10,000$. (Right) Map of normal forces obtained, for the same state, by applying the CDM with an additional 10% of contacts with respect to the real contact network. Force chains are correctly retrieved by the CDM, despite the error in building the contact network.

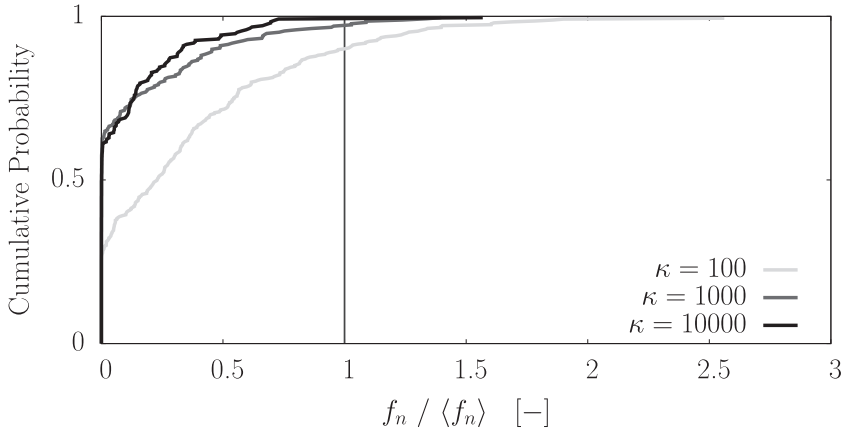

Fig. 8. Cumulative Distribution Function of normal forces carried by additional contacts for states with a 10% excess contacts for the three different simulations. Most of the contacts are shown to be carrying a weak normal force.

Please cite this article as: M. Tolomeo, V. Richefeu and G. Combe et al., An assessment of discrete element approaches to infer intergranular forces from experiments on 2D granular media, International Journal of Solids and Structures, https://doi.org/10.1016/j.ijsolstr.2019.01.010

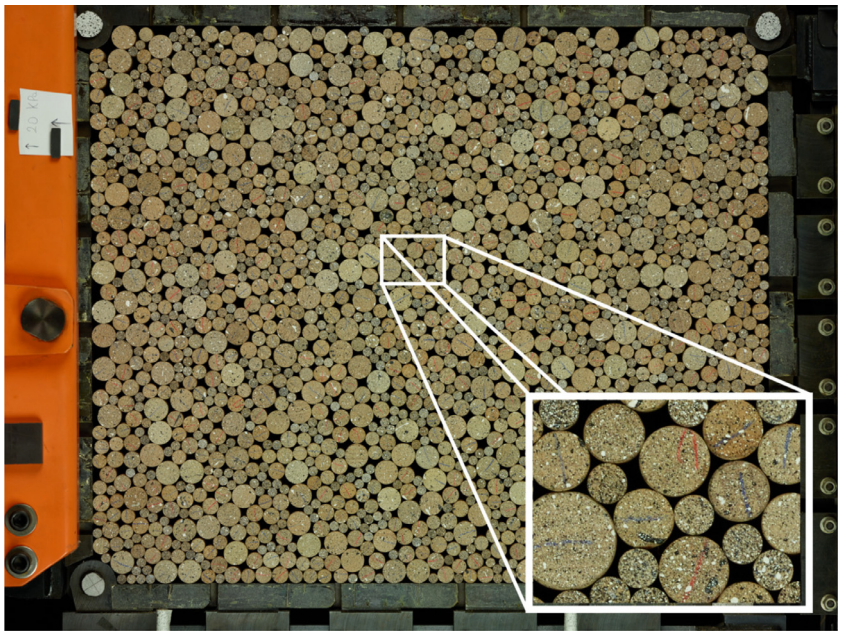

Fig. 9. (Colour online) Image of an isotropically compressed specimen in the $1\gamma 2\varepsilon$ device, with zoom on a small amount of grains to show the speckle pattern on their visible face. The frame is 556 mm × 459 mm.

reasonably assumed to be negligible. The assembly is composed of 6 cm long Schneebeli rods (Schneebeli, 1956); several materials or grain shapes can be adopted. In this case, an assembly of around 1800 ash wood circular rods was used; the four diameters employed were 8, 12, 14 and 20 mm. The material has an elastic modulus of 12 GPa; interparticle friction ϕ was measured with the same procedure as in Calvetti et al. (1997) and found to be equal to 24°($\pm 2°$). A single contact uniaxial compression test was performed to study the force-displacement response of the contact. The response was approximately fit by a bi-linear model, with a lower slope (stiffness) for the lowest range of normal forces ($f_n < 100$ N approximately). The response also showed some irreversibility when a second re-loading phase was applied after unloading the system. Due to this rather complex response, a unique value of k_n could not be easily determined from this experiment; at the same time, the assumption of more advanced contact models, such as the Hertzian law, would still be unable to reproduce such a behaviour. Therefore, it was decided to keep the simple linear model, and to adopt a different approach for calibrating k_n. A re-scaling procedure was carried out, consisting in computing a homogenised stress from estimated forces obtained with a guess k_n; then, a scalar quantity (the invariant p at the peak of the first compression cycle) was compared with the imposed pressure, and the ratio between the two values was used to multiply the guess value of k_n. The value of $k_n = 1.55 \times 10^6$ N/m obtained in this way – *i.e.*, by fitting the imposed loading – was very close to the one deduced from the linear fit of the force-displacement curve in the lowest range of normal forces. The tangential contact stiffness k_t was simply assumed to be equal to k_n.

Tests were carried out with different loading conditions: here, results will be presented only from an oedometer compression. The test was carried out by applying a constant strain rate in the vertical direction ($\dot{\varepsilon}_{yy}$) on the top arm, while lateral deformations were prevented; after reaching a normal stress of 200 kPa on the top side (σ_{yy}), an unloading phase was carried out, and the whole procedure was repeated for two cycles. Differently from the simulations in Section 3, the preparation of the sample did not involve the application of any confining load; by starting the test with $p \approx 0$ kPa, the corresponding stiffness level $\kappa = k_N/p$ turns out to be very high, although an exact estimation is not easy as we deal with very small pressures.

Both the image processing and Digital Image Correlation phases were performed by means of the software TRACKER (Combe and Richefeu, 2013; Richefeu et al., 2012). The aim of the image processing was to determine the geometry of the packing by assigning, to each rod (hereafter, grain or particle) a position (x, y) of its mass centre and a radius. With this aim, a binarised image was required; then, by computing for each pixel the distance from the closest black pixel (corresponding to a void), the centre of each grain could be identified, together with the grain's radius. Then, Particle Image Tracking (a specific DIC-based tool for discrete correlation) was carried out: a correlation pattern (a set of pixels) was defined for each grain (a concentric circle with a radius 20% smaller than the grain's one), and then "tracked" between two pictures by finding the maximum of a cross-correlation coefficient computed from the gray level of each pixel of the set. In order to create a unique pattern of gray values for each grain, a black-and-white speckle pattern was previously applied on the visible face of each rod.

Some typical measurement errors may come from several issues. Contact detection can be affected by the non-perfect roundness of the grains. For highly deformable materials, the measurement of strain inside the particle can help to understand whether there is a contact or not; but when the stiffness is high enough that no internal strain can be measured (with the given resolution), contact detection relies totally on the correct determination of particle centre and radius, hence it might be significantly affected by shape imperfections and measurement error. Hence, the number of contacts was verified by visually inspecting the assembly and adding/removing contacts that had been clearly misdetected. This confirmed that the error is typically lower than 10%, that was found to be a threshold below which the error does not affect the estimation of forces obtained with the CDM. An error is also associated to the measurement of displacements, and it was found to be equal to 0.01 ± 0.05 pixel (Combe and Richefeu, 2013), approximately corresponding to $0.7 \times 10^{-4} \pm 3.5 \times 10^{-4}$ m with the scale of the pictures taken during the above-mentioned tests.

Please cite this article as: M. Tolomeo, V. Richefeu and G. Combe et al., An assessment of discrete element approaches to infer intergranular forces from experiments on 2D granular media, International Journal of Solids and Structures, https://doi.org/10.1016/j.ijsolstr.2019.01.010

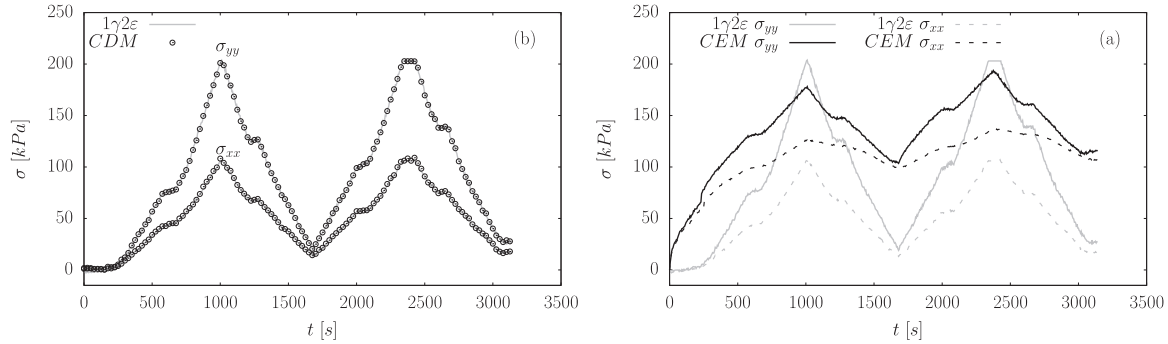

Fig. 10. (Left) Comparison between the $1\gamma 2\varepsilon$ macroscopic stress components and the Weber stress components computed from contact forces obtained by applying the CDM to an oedometer compression test. The evolution of stress components is retrieved with a very high precision. (Right) Comparison between the $1\gamma 2\varepsilon$ macroscopic stress components and the Weber stress components computed from contact forces obtained by applying the CEM to an oedometer compression test. The evolution of stress components is retrieved only from a qualitative point of view.

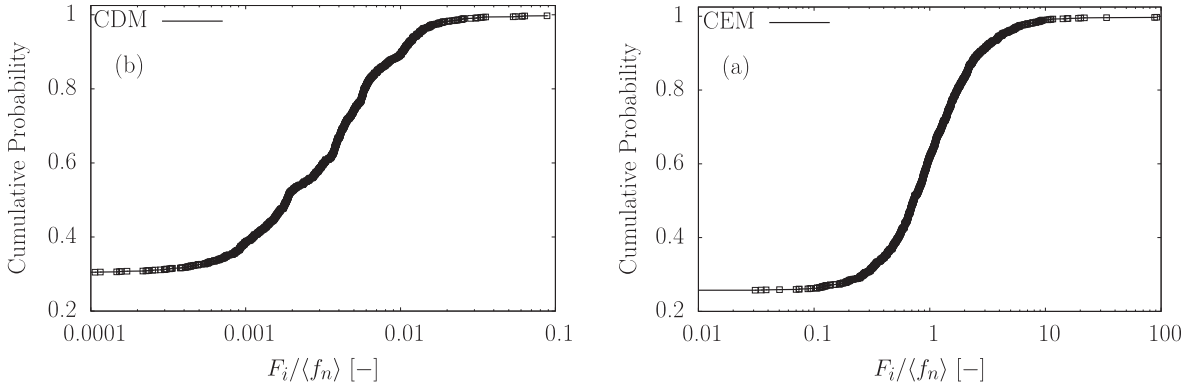

Fig. 11. (Left) Cumulative distribution function of the distance from equilibrium for all particles, at the end of the first loading cycle of the oedometer compression test, in the CDM solution. (Right) Cumulative distribution function of the distance from equilibrium for all particles, for the same state, in the CEM solution.

4.2. Results from both methods

The CEM makes use of the contact laws presented in Section 2.1. The determination of normal forces, since no overlap can occur in real experiments, relies on the equivalent measurement of a normal relative displacement that occurs when two compressed grains are deformed in an area localised around the contact point, while staying practically undeformed at a sufficient distance from the contact (which makes the correlation of a rigid pattern still possible as long as the pattern does not include the deformed area).

This incremental contact law, that writes $\delta f_n = k_n\ v_n\ \delta t$, introduces a linear relationship between the normal force increment and the contact normal relative displacement through the contact normal stiffness; based on this, a first, rough assessment of the influence of measurement error on the estimation of normal forces for the presented test can be obtained by simply multiplying the displacement error associated to the Digital Image Correlation algorithm (as in Section 4.1) and the stiffness that was estimated from a specific compression test on a single contact. This estimation gave a maximum error, in terms of normal force, of approximately 50 N, in the same order of magnitude of the average normal force, estimated as $\approx$70 N for a pressure of 100 kPa.

With such a large error, the estimation of forces could not be expected to be realistic. In order to have a more reliable estimation of forces, one should either increase the accuracy or the resolution of the measurements, or decrease the contact stiffness (or both at the same time).

On the other hand, CDM's solution is expected to be much more realistic and reliable, thanks to the higher robustness of the CDM with respect to measurement error, as shown in Section 3.2. The evaluation of the quality of the force estimation can be done on different levels: on a macroscopic point of view, by building a homogenised stress from contact forces, that allows a comparison also with the experimental data, as the macroscopic stress is measured by the machine at any stage of the test; on a microscale level, maps of normal forces are a typical result from which, based on geometrical patterns that are expected to appear when the force network is well retrieved (such as chain-like and ring-like structures), the accuracy of the solution can be deduced; finally, since the test is performed in quasi-static loading conditions, the satisfaction of particle equilibrium is another criterion that can be exploited to give an assessment of the quality of the solution in forces.

The homogenised stress over a volume V can be computed from contact forces as a sum, over all contacts α, of the dyadic product between the force $\mathbf{f}^\alpha$ and the branch vector $\boldsymbol{\ell}^\alpha$ connecting the two particles centres, following the expression by Weber (1966):

$$\sigma_{ij} = \frac{1}{V}\sum_{\alpha=1}^{N_c} f_i^\alpha \ell_j^\alpha \tag{4}$$

In the CEM case, such an estimation of the homogenised stress gives a first confirmation of how significant the effect of measurement error is for this method, with the current measurement resolution and the given deformability of the material: the evolution of σ_{yy} and σ_{xx} (vertical and horizontal normal stresses, respectively) does not reproduce the evolution of the corresponding components as measured by the machine throughout the test (Fig. 10b). The set of forces obtained with the CDM gives a homogenised stress that

Please cite this article as: M. Tolomeo, V. Richefeu and G. Combe et al., An assessment of discrete element approaches to infer intergranular forces from experiments on 2D granular media, International Journal of Solids and Structures, https://doi.org/10.1016/j.ijsolstr.2019.01.010

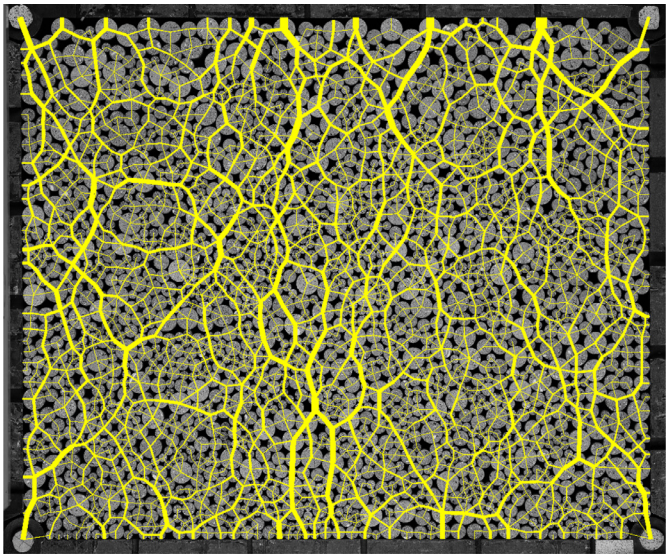

Fig. 12. (Colour online) Map of normal contact forces obtained via the CDM at the end of the first loading cycle of the oedometer compression test. Line thickness of the branch vectors is proportional to normal force intensity. Here, force chains clearly appear, mainly along the vertical direction, as expected. The largest normal force is around 1000 N.

reproduces much better the real, macroscopic one (Fig. 10a): the evolution is clearly retrieved both on a qualitative point of view and on a quantitative one.

Fig. 11 shows the statistics of distance from static equilibrium, for all particles, at the end of the first loading phase of the oedometer compression test, as obtained respectively from the CEM solution (Fig. 11b) and the CDM one (Fig. 11a). The distance from equilibrium is defined as the ratio between the magnitude of the unbalanced force on each grain (F_i) and the mean normal force over the whole network ($\langle f_n \rangle$). Such a distance is found to be equal to 1.285 ± 3.489 for the CEM solution, and 0.003 ± 0.006 for the CDM case, showing that the CDM provides a solution much closer to equilibrium than the CEM.

In the map of CDM-computed normal contact forces for a state at the end of the compression phase (Fig. 12), force chains appear clearly, and they tend to be aligned along the vertical direction. A quantitative assessment of the accuracy of this estimation is not possible at this stage; however, some conclusions can be inferred on how close to reality is this solution, based on the results of the validation phase. Since the measurement error, consisting in a possible bad contact detection, has been proven to have a limited influence, the main source of error lies in the non-uniqueness of the solution: based on the estimation of κ in experiments (125 at peak, 500 at $p = 50$ kPa), it is expected that estimated forces have a Pearson correlation with real forces in the range $0.70 - 0.85$.

5. Conclusion and perspectives

In granular materials, the combination of measurements of the geometrical arrangement of the packing and of the rigid body particle-scale kinematics with numerical DEM-based approaches seems a promising way to inferring interparticle contact forces, independently of the used material and its stiffness.

To this end, two different approaches were proposed. The validation phase, that consisted in extracting input information from ideal experiments (MD simulations) and trying to retrieve the set of contact forces, showed a good correspondence between the estimated solution and the real one; at the same time, it highlighted some peculiar aspects of the two methods, as well as the limitations that were observed once more in the successive application phase.

The contact elasticity method (CEM), being based on the simple assumption that forces can be directly assessed from measurements of particle kinematics, relies on the accuracy of such measurements, as well as on the time resolution of the data acquisition; moreover, particle equilibrium (that should be verified as long as the loading is quasi-static) is never accounted for in this method. The Contact Dynamics-based method (CDM) has the intrinsic limitation of the force indeterminacy related to the non-uniqueness of the solution. However, it is not affected very much by measurement error and it has the advantage of providing an estimation of forces simply from a snapshot of a granular system, neglecting its previous evolution.

Force indeterminacy remains the main source of error when using the CDM for force inference; however, it was shown (Unger and Kertèsz, 2003) that generally the fluctuations of forces do not significantly change the force network structure. The effect of interparticle friction is also to be accounted for: as shown by Unger and Kertèsz (2003), the largest indeterminacy is typically found for $\mu = 0.1$, above which a significant decrease is observed; in this case, with $\mu \approx 0.45$, indeterminacy can be considered to be relatively low.

However, local deformations can be employed to further decrease such variability and get a more accurate solution. This could be done through the CEM, provided that the measurement error is reduced by either increasing the measurement accuracy or the deformability of the material.

Other procedures to reduce the indeterminacy issue can be implemented. In particular, force estimation would certainly benefit from taking into account the history of the packing. As previously explained, this is not strictly necessary according to the formulation of the method; however, as it has been shown by McNamara et al. (2005), force indeterminacy is actually linked with the different possible histories. Since history is basically encoded in the choice of the initial guess solution, possible strategies to account for it include, *e.g.*, using the solution of a state as an initial guess for the next state.

Here, we showed an application to a 2D case; however, the CDM can be applied to a 3D ideal assembly (*e.g.*, spheres) without any conceptual limitation. A higher complexity might come from problems in the detection of contact points and contact orientations in the case of a non-ideal packing.

In a next future, applications of both methods are planned on different materials (*e.g.*, aluminium, polyurethane), in order to test the methods for different levels of particle stiffness. A combination of the CDM with other methods could be a way to improve its result; at the same time, referring to other methods as benchmarks could be a way to assess the precision of the obtained solution. In addition to this, foreseeable technological advances in the grain-scale characterization are something that both methods could benefit from.

The approach followed in the CDM, consisting of using only granular arrangement and boundary conditions for the estimation of forces, will be pursued also through a quasi-static method that aims to find a set of forces, for a granular assembly in stable equilibrium, satisfying at the same time the criteria of static and plastic admissibility (Roux and Combe, 2011).

Conflict of interests

The authors declare that there is no conflict of interests associated with this publication.

Please cite this article as: M. Tolomeo, V. Richefeu and G. Combe et al., An assessment of discrete element approaches to infer intergranular forces from experiments on 2D granular media, International Journal of Solids and Structures, https://doi.org/10.1016/j.ijsolstr.2019.01.010

Acknowledgements

The first author thanks the LabEx Tec 21 (Investissements d'Avenir, Grant Agreement No. ANR-11-LABX-0030) for full financial support of his PhD, which this work is part of.

References

Andrade, J.E., Avila, C.F., 2012. Granular element method (GEM): linking inter-particle forces with macroscopic loading. Granul. Matt. 14, 51–61.
Calvetti, F., Combe, G., Lanier, J., 1997. Experimental micromechanical analysis of a 2D granular material: relation between structure evolution and loading path. Mech. Cohes.-Friction. Mater. 2, 121.
Combe, G., Richefeu, V., 2013. TRACKER: A particle image tracking (PIT) technique dedicated to nonsmooth motions involved in granular packings. AIP Conf. Proc. 1542, 461.
Cundall, P., Strack, O., 1979. A discrete numerical model for granular assemblies. Géotechnique 29(1), 47–65.
Dantu, P., 1957. Contribution à l'étude mécanique et géométrique des milieux pulvérulents. In: Proceedings of the 4th International Conference on Soil Mechanics and Foundation Engineering. Butterworth Scientific, London.
Doreau-Malioche, J., Combe, G., Viggiani, G., Toni, J.B., 2018. Shaft friction changes for cyclically loaded displacement piles: an X-ray investigation. Géotech. Lett. 8, 1–28.
Hurley, R.C., Hall, S.A., Andrade, J.E., Wright, J., 2016. Quantifying interparticle forces and heterogeneity in 3D granular materials. Phys. Rev. Lett. 117, 098005.
Hurley, R.C., Marteau, E., Ravichandran, G., Andrade, J.E., 2014. Extracting inter-particle forces in opaque granular materials: beyond photoelasticity. J. Mech. Phys. Solids 63, 154.
Joer, H., Lanier, J., Desrues, J., Flavigny, E., 1992. $1\gamma 2\varepsilon$: A new shear apparatus to study the behavior of granular materials. Geotech. Test. J. 15, 129.
Karatza, Z., Andò, E., Papanicolopulos, S.A., Ooi, J.Y., Viggiani, G., 2017. Evolution of deformation and breakage in sand studied using X-ray tomography. Géotechnique 68, 1–11.
Majmudar, T.S., Behringer, R.P., 2005. Contact force measurements and stress-induced anisotropy in granular materials. Nature 435, 1079.
Marteau, E., Andrade, J.E., 2017. A novel experimental device for investigating the multiscale behavior of granular materials under shear. Granul. Matt. 19, 1–12.
McNamara, S., Herrmann, H., 2004. Measurement of indeterminacy in packings of perfectly rigid disks. Phys. Rev. E. 70, 1–12.
McNamara, S.C., García-Rojo, R., Herrmann, H.J., 2005. Indeterminacy and the onset of motion in a simple granular packing. Phys. Rev. E. 72 (2), 1–12.
Moreau, J.J., 2004. An Introduction to Unilateral Dynamics. In: Frémond, M., Maceri, F. (Eds.), Novel approaches in civil engineering. Springer-Verlag, pp. 1–46.
Mueth, D., Jaeger, H.M., Nagel, S.R., 1998. Force distribution in a granular medium. Phys. Rev. E. 57, 3164–3169.
Radjai, F., Jean, M., Moreau, J.J., Roux, S., 1996. Force distributions in dense two-Dimensional granular systems. Phys. Rev. Lett. 77, 274.
Radjai, F., Richefeu, V., 2009. Contact dynamics as a nonsmooth discrete element method. Mech. Mater. 41, 715–728.
Radjai, F., Wolf, D., Jean, M., Moreau, J.J., 1998. Bimodal character of stress transmission in granular packings. Phys. Rev. Lett. 80, 61–64.
Richefeu, V., Combe, G., Viggiani, G., 2012. An experimental assessment of displacement fluctuations in a 2D granular material subjected to shear. Géotechnique Letters 2, 113.
Roux, J.N., 2000. Geometric origin of mechanical properties of granular materials. Phys. Rev. E. 61, 6802–6836.
Roux, J.N., Combe, G., 2011. Quasistatic Methods. In: Radjai, F., Dubois, F. (Eds.), Discrete-element Modeling of Granular Materials. Wiley-Iste, chapter 3, pp. 83–116.
Schneebeli, G., 1956. Une analogie mécanique pour les terres sans cohésion. Comptes Rendus de l'Academie des Sciences 243, 125–126.
Unger, T., Kertèsz, J., 2003. Frictional indeterminancy of forces in hard-disk packings. Int. J. Mod. Phys. B. 17, 5623–5630.
Weber, J., 1966. Recherches concernant les contraintes intergranulaires dans les milieux pulvérulents. Bulletin de liaison des ponts et chaussées 20, 1–20.

Please cite this article as: M. Tolomeo, V. Richefeu and G. Combe et al., An assessment of discrete element approaches to infer intergranular forces from experiments on 2D granular media, International Journal of Solids and Structures, https://doi.org/10.1016/j.ijsolstr.2019.01.010